

NORSAR Scientific Report No. 2-91/92

Semiannual Technical Summary

1 October 1991 – 31 March 1992

Kjeller, May 1992

APPROVED FOR PUBLIC RELEASE, DISTRIBUTION UNLIMITED

7.4 Travel time corrections for a 3-D velocity model beneath the NORSAR array

Introduction

For the purpose of improving the event location capability of the NORSAR array, Berteussen (1974) constructed a time correction table from average arrival time residuals for 94 different incident P-wave directions, and Berteussen (1976) concluded that almost all of the observed time residuals across the array can be corrected for by using this table, and therefore the residuals have their origin in the upper mantle and crust beneath the array. Time corrections are computed from this table by linear interpolation between nodes in incident slowness space, and this table is the one most frequently used for time corrections at NORSAR. Due to the very nonuniform distribution of earthquakes, interpolation is unavoidable in this kind of correction procedure. However, if the observed residuals could be explained in terms of subsurface structures, another type of correction table could be made by forward modeling the effects of such structures.

In one of the first applications of travel time tomography in seismology, Aki et al (1977) inverted the time residuals of the NORSAR time correction table for P-wave velocity perturbations beneath the array, and a similar experiment has been done with a slightly different and larger data set. Systematic analysis of this data set revealed the significant influence of diffraction effects like focusing and defocusing from low and high velocity zones, and diffraction effects have been taken into account, in a first-order approximation, using a reformulation of diffraction tomography (Ødegaard and Doornbos, 1992). Synthetic data have been computed for the velocity models produced by ordinary seismic tomography and by diffraction tomography, and from these data correction tables have been constructed. There is no further need for interpolation when using these correction tables. Some results concerning these tables are presented.

Tomography

The basis of ordinary seismic tomography (ST) is the simple relation:

$$\delta\tau = \int_{ray} \delta s \cdot d\sigma \quad (1)$$

This equation states that a change in travel time is due to a slowness perturbation $\delta s = -v^{-2}\delta v$ along the ray, and it predicts a time shift of a reference pulse u_0 :

$$\mathbf{u}(\mathbf{x}, t) = \mathbf{u}_0(\mathbf{x}, t - \delta\tau) \quad (2)$$

Eq. (2) can be viewed as a smooth approximation since it is a valid expression if the slowness perturbation δs varies smoothly within the medium. The reformulation of diffraction tomography (DT), as derived by Doornbos (1992), predicts a diffraction term as a perturbation to the time-shifted reference pulse (which is the smooth approximation of ST):

$$\mathbf{u}(\mathbf{x}, t) = \mathbf{u}_0(\mathbf{x}, t - \delta\tau) + \int_V \mathbf{B} \cdot \nabla \cdot \delta s \cdot dV \quad (3)$$

This reformulation alleviates some of the fundamental problems of both seismic and diffraction tomography. The velocity structure beneath the NORSAR array has been modeled down to a depth of 129 km using ST, Eq. (1), and using DT in the frequency domain with short-period (SP) subarray phase and amplitude residuals from 115 events, and long-period (LP) phase residuals from 31 events. Synthetic data can be computed after forward modeling using Eq. (1) (ray travel times) and Eq. (3) (synthetic wave recordings). Further details concerning these methods are given by Ødegaard and Doornbos (1992).

Correction tables

SP P-wave time correction tables have been constructed for the ST model, using Eq. (1) (ray travel time), and the DT model, after using Eq. (3) with a 1 Hz damped sine reference pulse and iterative correlation between the synthetic array beams and subarray beams for 1.5 s time windows. The two low-pass filtered time correction tables for subarray 01A are plotted in Figs. 7.4.1 and 7.4.2, for slowness values less than 0.08 s/km, corresponding to epicenter distances greater than 30°. Figs. 7.4.3 and 7.4.4 display the predicted time residuals versus the observed time residuals for the two time correction tables and the 115 events. The ray travel time table constructed from the ST model predicts the observed time residuals slightly better than the DT correction table; the normalized squared error is 12% for the ST table and 19% for the DT table, and the correlation coefficient is 0.94 for the ST table and 0.91 for the DT model. For the purpose of constructing a time correction table, the ST model provides the best results. The ST model is given in Table 7.4.1. However, the DT model predicts the phase and amplitude spectra of the data significantly better than the ST model; the normalized squared error for the phase spectra is 20% for the ST model and 10% for the DT model, and the normalized squared error for the amplitude spectra is 75% for the ST model and 55% for the DT model (Ødegaard and Doornbos, 1992).

E. Ødegaard, Univ. of Oslo

References

- Aki, K., A. Christoffersson and E.S. Husebye (1977): Determination of the three-dimensional structure of the lithosphere, *J. Geophys. Res.*, 82, 277-296.
- Berteussen, K.-A. (1974): NORSAR location calibrations and time delay corrections. *Sci. Rep. 2-73/74*, NTNF/NORSAR, Kjeller, Norway.
- Berteussen, K.-A. (1976): The origin of slowness and azimuth anomalies at large arrays, *Bull. Seism. Soc. Am.*, 66, 719-741.
- Doornbos, D.J. (1992): Diffraction and seismic tomography, *Geophys. J. Int.*, 108, 256-266.
- Ødegaard, E. and D.J. Doornbos (1992): Seismic diffraction tomography of array data, *J. Geophys. Res.*, in press.

Layer 4 (54-79km) $v_0 = 8.1$ km/s

=	=	=	=	-0.4	0.1	-1.2	-4.2	1.7	-3.6	-0.5	=	=
=	=	=	-0.5	1.6	0.8	-0.3	-1.4	-1.2	0.4	2.4	=	=
=	0.2	0.9	-0.9	1.3	1.4	-2.1	1.1	0.8	-1.4	-2.6	-1.6	-0.3
=	2.4	-1.0	-0.2	-2.3	-2.0	-0.2	0.5	0.0	1.4	-1.5	-2.3	-6.0
1.3	-2.0	0.4	-3.0	-3.4	0.6	-0.6	-1.7	-0.3	0.6	2.2	2.2	-3.3
3.9	-4.0	-1.0	-0.9	0.9	3.8	1.2	-0.1	-2.1	-0.4	3.0	5.1	-2.7
0.3	-1.7	-0.3	-1.3	0.0	1.2	0.3	-1.3	-0.5	0.4	0.2	5.2	2.1
2.0	-0.3	-1.3	-2.6	0.2	0.5	-1.5	-0.5	1.5	0.0	0.1	5.9	-0.4
2.0	1.8	-1.5	-3.2	-2.6	-2.2	0.7	3.3	1.5	1.8	-1.3	4.0	0.4
=	-2.0	1.9	-2.7	-5.2	-3.6	-2.0	1.3	5.4	3.4	-1.4	3.2	1.3
=	-0.3	-0.7	-4.0	-1.3	-2.4	-3.8	2.6	6.8	1.4	3.5	5.8	=
=	=	=	-0.2	0.7	1.2	2.5	-0.1	-2.3	2.2	4.6	0.7	=
=	=	=	=	=	0.5	=	2.2	=	=	1.1	=	=

Layer 5 (79-104km) $v_0 = 8.1$ km/s

=	=	0.0	-0.4	-1.1	-0.5	0.4	-0.1	-1.5	-1.4	-1.5	=	=
=	-0.3	-0.4	4.6	3.8	0.8	-1.7	-0.3	-1.9	-1.8	-1.8	-1.6	=
0.7	0.4	1.5	1.0	2.8	-1.6	0.2	-0.6	0.8	0.4	-1.1	-0.2	-1.5
=	2.2	-0.3	0.3	0.5	-2.4	-1.2	0.6	3.1	0.3	1.1	0.7	-3.4
1.2	1.2	-1.0	-1.5	-1.8	-2.4	-1.3	0.4	2.5	3.7	4.1	1.7	-1.2
2.2	-1.8	-3.1	-0.5	-3.3	-3.2	-2.9	-0.5	2.3	6.4	5.4	5.1	-1.1
-2.6	-2.2	-3.6	-2.3	0.6	-2.4	-2.8	-1.7	0.9	5.0	3.4	4.8	-0.2
-2.0	-6.7	-3.5	-2.5	-0.9	-2.5	-2.7	0.4	0.7	0.7	4.9	3.8	3.0
0.0	0.2	-3.3	-1.2	-1.7	-1.0	-2.3	-1.4	-0.1	2.0	3.6	3.4	8.2
0.9	-0.9	-0.5	0.2	1.2	-2.6	-1.5	-0.6	0.9	-3.3	1.9	3.6	7.7
-0.2	-3.2	-2.1	2.6	0.5	-0.2	0.5	0.0	-2.0	-2.1	-0.2	2.8	3.1
=	-1.3	0.3	-0.2	1.8	1.7	3.0	0.7	-4.2	-5.0	1.1	0.3	3.6
=	=	=	-1.3	0.1	2.5	-0.6	-0.6	1.1	-0.4	3.3	2.5	=

Layer 6 (104-129km) $v_0 = 8.1$ km/s

=	1.0	-0.6	2.6	0.0	0.5	0.3	-2.0	-0.7	-3.3	-0.4	0.1	-0.8
=	5.8	9.2	-1.1	1.8	3.3	1.7	0.3	-0.4	-1.6	-0.9	2.0	0.0
2.1	5.0	2.9	3.3	0.4	4.9	5.8	3.6	0.4	2.1	1.0	0.7	0.8
0.8	3.9	5.4	0.7	2.2	1.5	2.6	3.1	2.8	3.1	3.6	2.1	-0.1
1.0	0.7	-3.8	-3.5	-1.4	-1.6	-2.6	0.2	3.7	6.1	5.4	3.2	1.2
0.3	-2.4	-4.6	-4.7	-5.7	-3.7	-5.3	-3.0	3.0	6.1	6.0	4.7	-0.1
-0.8	-2.7	-5.1	-9.6	-8.3	-3.6	-7.4	-3.4	-0.6	4.9	6.3	4.5	3.2
-1.0	-3.7	-2.6	-6.2	-3.4	-4.1	-1.6	-3.2	-0.5	2.0	3.2	2.8	5.9
0.1	-0.8	0.1	-2.8	-3.0	-1.6	1.7	-1.1	-1.7	-2.5	1.2	3.7	5.4
-2.5	-1.6	-0.2	-0.6	0.7	5.5	3.8	-1.4	-3.9	-4.3	-0.9	2.6	4.4
-3.2	0.2	-1.1	2.4	2.7	6.8	2.6	-1.3	-4.4	-7.9	-2.5	2.7	3.3
-1.9	0.1	1.2	1.7	3.3	7.8	2.1	-3.3	-4.9	-5.2	-1.5	-0.1	4.1
=	0.0	0.2	0.5	4.4	1.4	3.7	-0.6	-2.6	-3.9	-2.0	0.0	1.8

Table 7.4.1 (cont.) (Page 2 of 2).

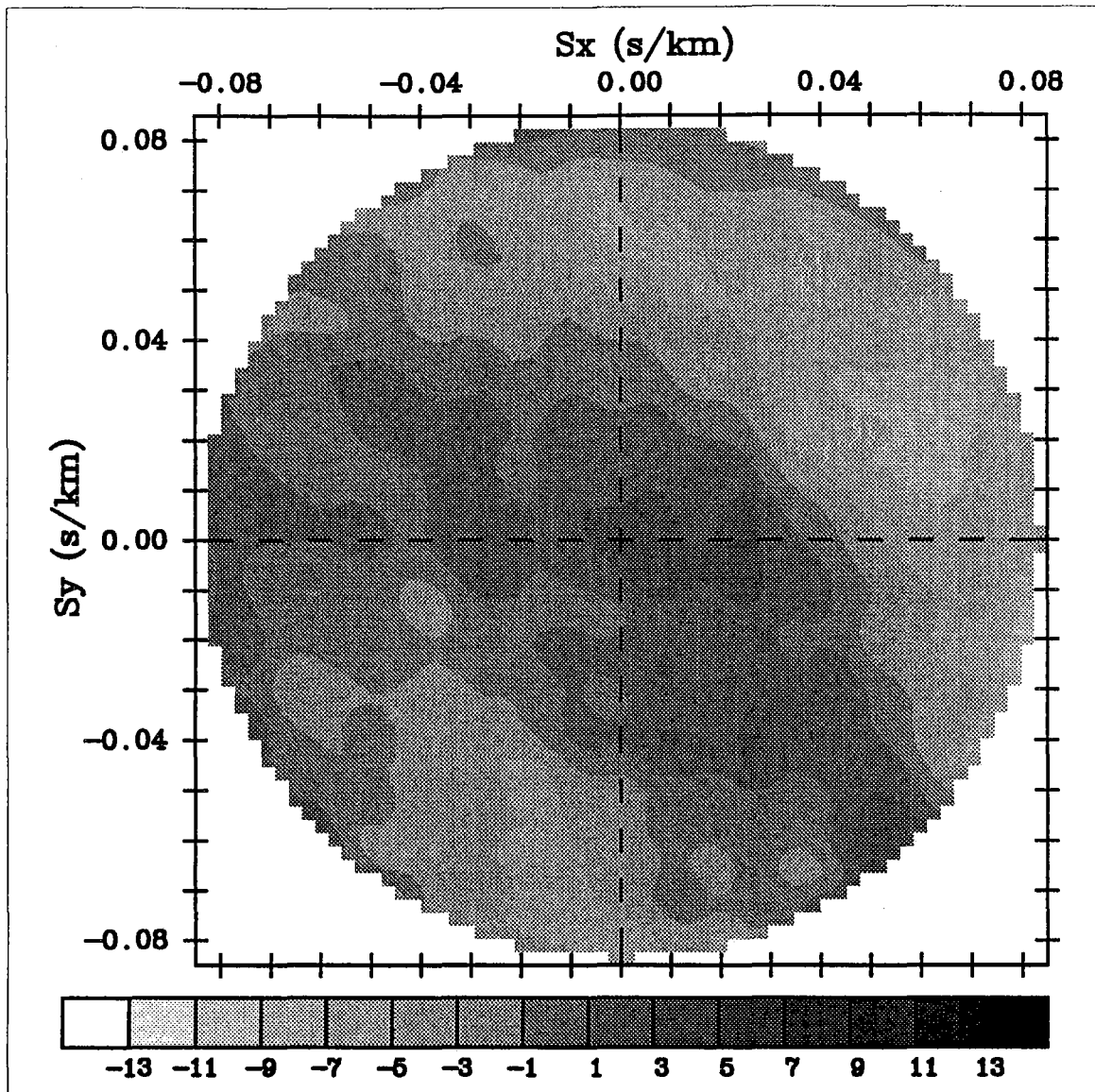


Fig. 7.4.1. The low-pass filtered SP P-wave ray travel time corrections at subarray 01A, for the ST model (given in Table 7.4.1) and for slowness values less than 0.08 s/km. The SP sampling rate is 20 Hz, and the time delay is given in units of 0.05 s.

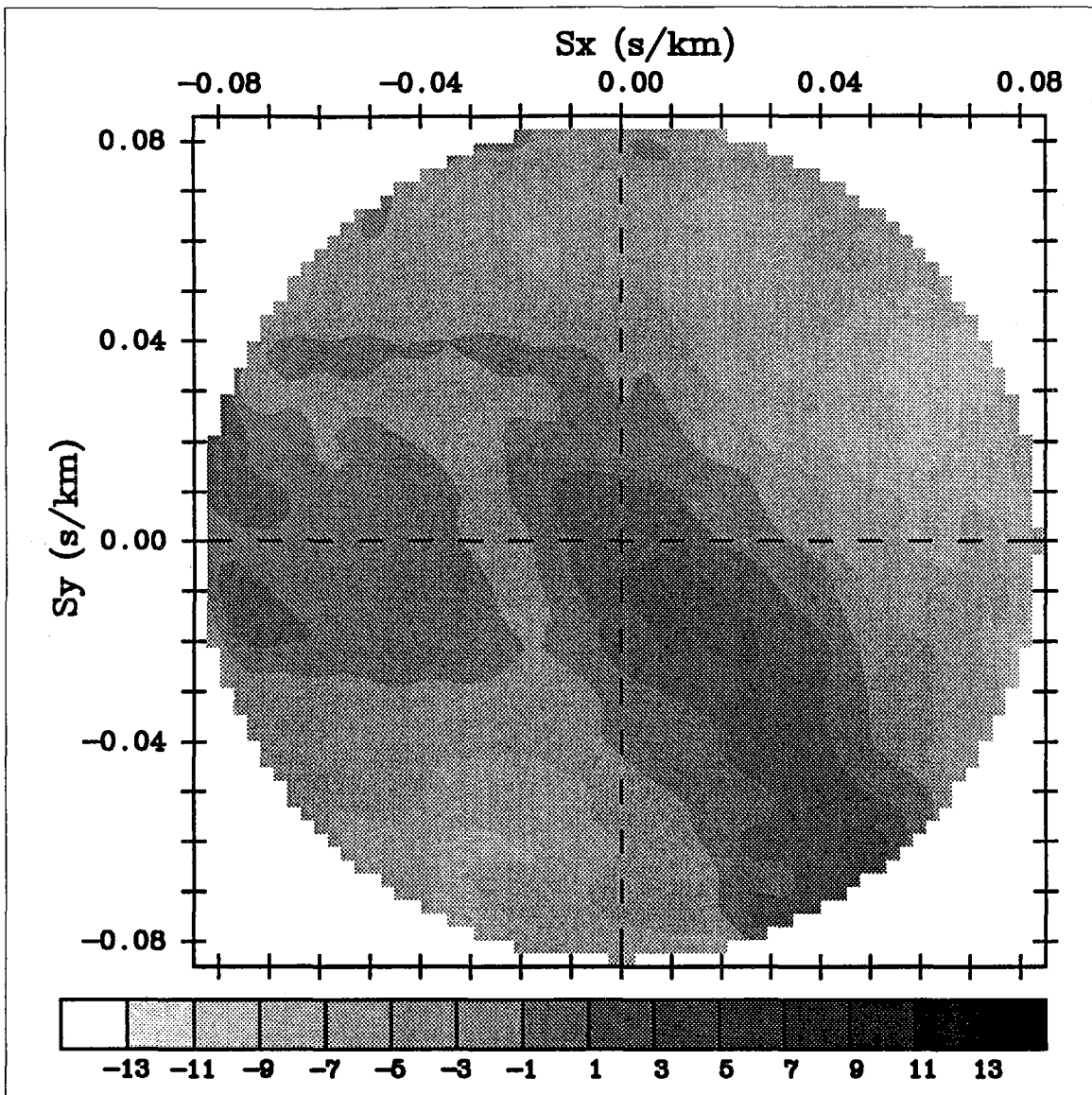


Fig. 7.4.2. The low-pass filtered SP P-wave time corrections at subarray 01A for the DT model and a 1 Hz damped sine reference pulse.

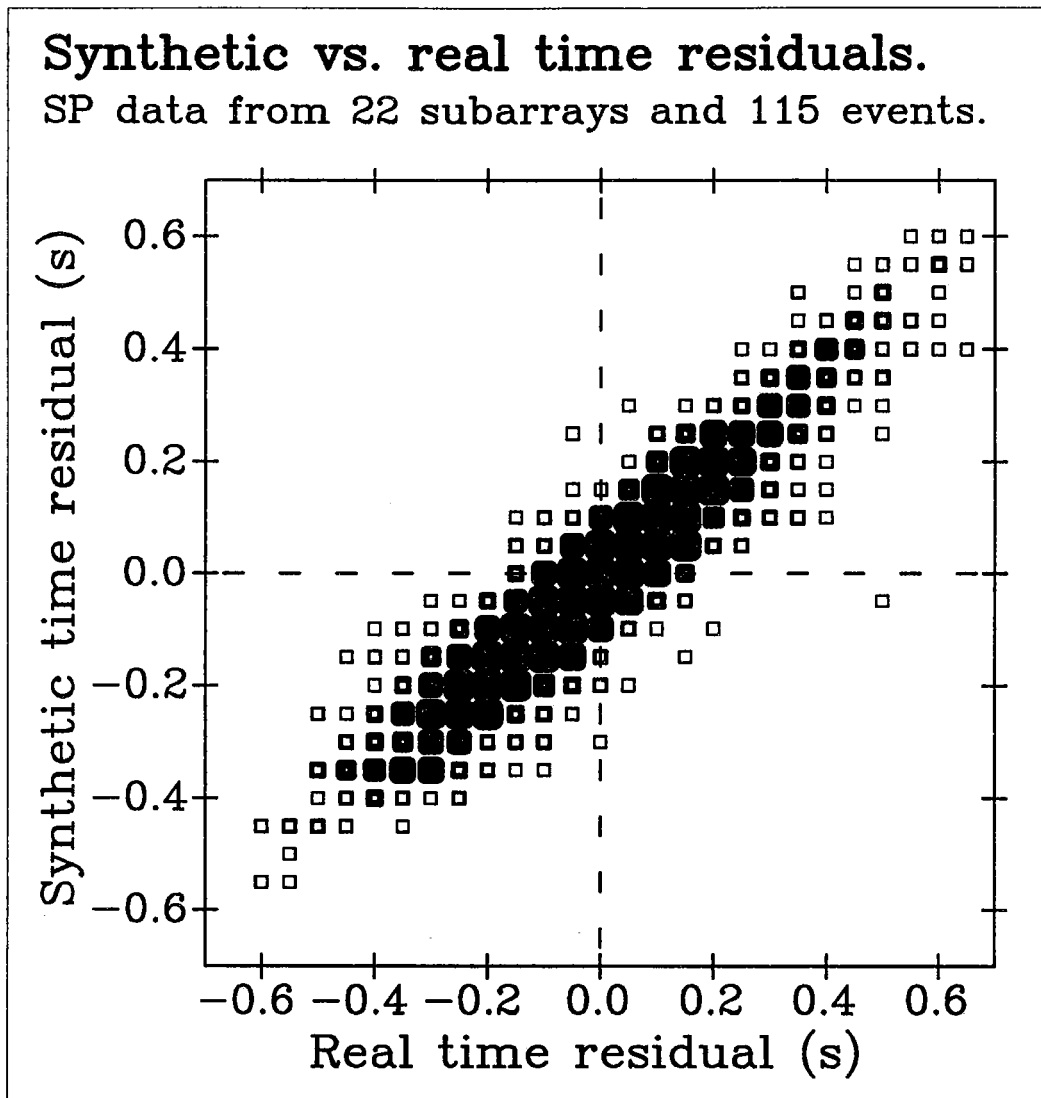


Fig. 7.4.3. Predicted SP P-wave ray travel time residuals versus observed time residuals for the ST model. Symbol size is proportional to number of data.

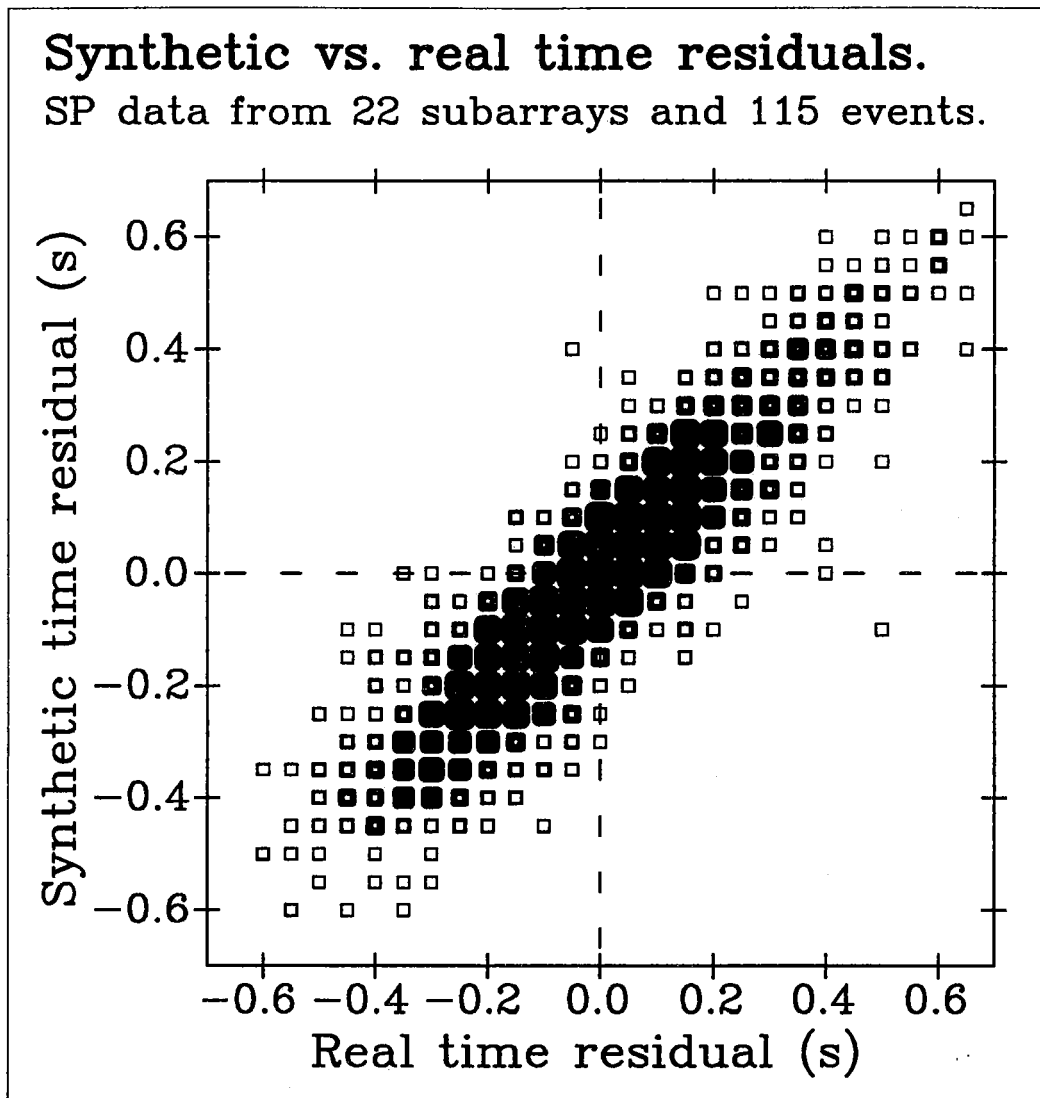


Fig. 7.4.4. Predicted SP P-wave time residuals versus observed time residuals for the DT model and a 1 Hz damped sine reference pulse.